Electron Detection for Compton Polarimetry

Michael H. McDonald

Supervisor: Dr. J. Martin

Honours Thesis

April 28, 2008

Abstract

The Qweak experiment at Jefferson Lab is an example of an experiment that requires the polarization of a high-energy electron beam be known to 1%. A non-invasive and continuous way to determine the polarization is through the use of Compton polarimetry.

In Compton polarimetry, a beam of electrons of unknown polarization is struck by photons from a laser of known polarization. Scattered electrons and scattered photons are detected, and the polarization of the beam can be determined based on the detection. In Qweak, the detector used to sense scattered electrons will be made of synthetic diamond.

In this thesis, characterization of diamond detectors was studied using radioactive sources. Theory of Compton polarimetry, design and operation of detectors, and results of various tests will be discussed.

Author: Michael H. McDonald

Thesis Supervisor: J. Martin
Thesis Committee: D. Vincent and S. Dannefaer

Contents

List of Figures

Chapter 1

Compton Polarimetry

The process of a photon scattering from a free electron is called the Compton effect. Both of these particles carry spin angular momentum. The relative alignment or anti-alignment of the spins forms the foundation for Compton polarimetry.

1.1 Compton Scattering Kinematics

Consider a beam of electrons moving along the z-axis. An electron in the beam will have the four-momentum $p^\mu = (E, 0, 0, p)$ associated with it. Consider also, an incoming photon striking the electron at an angle θ to the z-axis. The photon will have associated with it, a four-momentum $k^\mu = (k, -k\sin\theta, 0, -k\cos\theta)$. This geometry is shown in Figure 1.1. Units are used such that the speed of light $c = 1$.

After the interaction, the electron loses some energy by the Compton effect and becomes deflected from the main beam by an angle ϕ_e from the z-axis. The photon, having gained energy departs at angle ϕ_γ with new four-momentum $k^{\mu'} = (k', k'\sin\phi_\gamma, 0, k'\cos\phi_\gamma)$.

Now, applying conservation of four-momentum, that is, $p^\mu + k^\mu = p^{\mu'} + k^{\mu'}$, we arrive at the following result for the energy of the scattered photon:

$$k' = k\frac{E + p\cos\theta}{E + k - p\cos\phi_\gamma + k\cos(\theta - \phi_\gamma)} \tag{1.1}$$

The energy of the electron is thus,

$$E' = E + k - k' \tag{1.2}$$

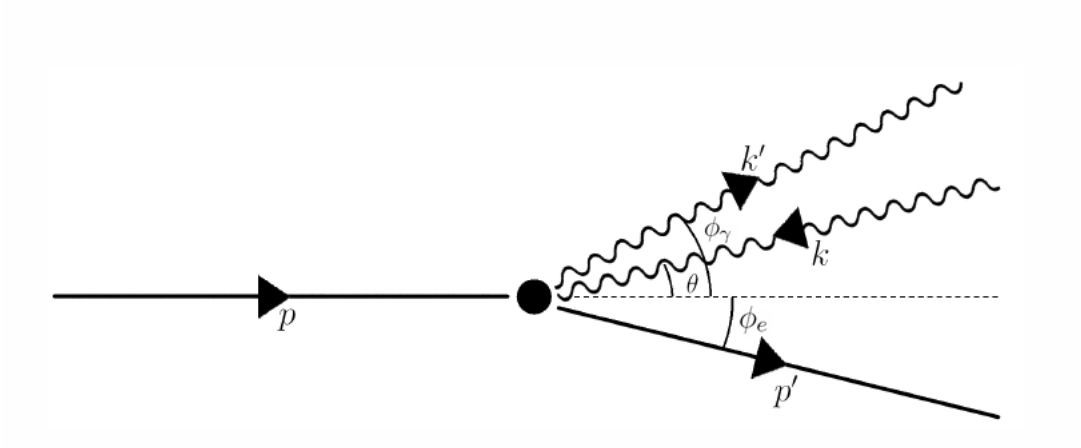

Figure 1.1: Compton Scattering

There exists a maximum scattered photon energy, this is the Compton edge. The maximum occurs when $\phi_\gamma = 0$. At the Compton edge, the outgoing electron has its minimum energy. To increase the likelihood of Compton scattering, the experiment is arranged such that $\theta \approx 0$. Using $\phi_\gamma = \theta = 0$, the maximum scattered photon energy is

$$k'_{max} = k\frac{E+p}{E+2k-p} \tag{1.3}$$

1.2 Asymmetry and Cross-sections

The basis of Compton polarimetry is an asymmetry in the number of events detected for each relative helicity state.

This experimental asymmetry is defined as

$$A_{exp} = \frac{n^+ - n^-}{n^+ + n^-} \tag{1.4}$$

Here n^+ and n^- are the number of events detected for each relative helicity state.

The polarization of the beam, P_e, is then calculated using:

$$A_{exp} = P_e P_\gamma A_\ell \tag{1.5}$$

where P_γ is the known polarization of the laser. A_ℓ is the theoretical asymmetry which will now be described.

1.2.1 Compton Cross-Section

The differential cross section measures the probability of an interaction between the electron and photon. The cross section can be calculated in quantum electrodynamics from the Feynman diagrams for Compton scattering shown in Figure 1.2.

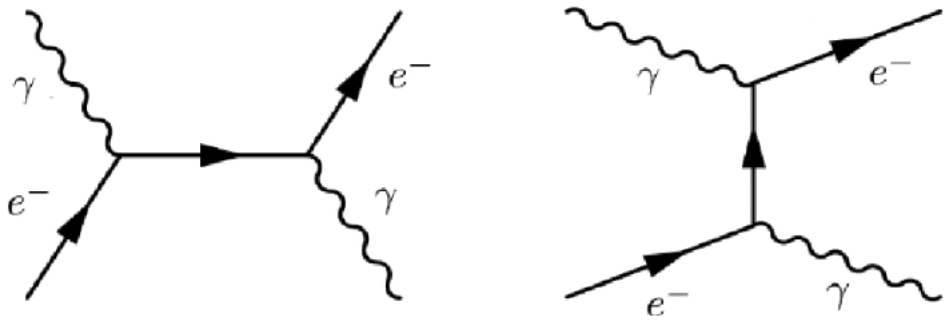

Figure 1.2: The two leading order Feynman diagrams for Compton Scattering

For a laser beam with incident angle $\theta = 0$, the differential unpolarized cross section is given by [3],

$$\frac{d\sigma}{d\rho} = 2\pi r_0^2 a \left[\frac{\rho^2(1-a)^2}{1-\rho(1-a)} + 1 + \left(\frac{1-\rho(1+a)}{1-\rho(1-a)} \right)^2 \right] \tag{1.6}$$

Where r_0 is the classical radius of the electron, ρ is the photon energy relative to the maximum (i.e. $\frac{k'}{k'_{max}}$), and a is a kinematical parameter defined as $a = \frac{1}{1+\frac{4kE}{m_e^2}}$.

To get the total differential cross section, $\frac{d\sigma^\pm}{d\rho}$ requires the average of the polarized and unpolarized cross sections, that is, $\frac{d\sigma^+}{d\rho}$ is the cross section for electron and photon polarized parallel, and $\frac{d\sigma^-}{d\rho}$ is the cross section for anti-parallel polarizations.

The theoretical asymmetry is given by

$$A_\ell = \frac{\sigma^+ - \sigma^-}{\sigma^+ + \sigma^-} \tag{1.7}$$

where $\sigma^\pm$ means $\frac{d\sigma}{d\rho}^\pm$. The functional form of A_ℓ as a function of unpolarized cross section is [3]

$$A_\ell = \frac{2\pi r_0^2 a}{\frac{d\sigma}{d\rho}}(1-\rho(1+a))\left(1-\frac{1}{(1-\rho(1-a))^2}\right) \tag{1.8}$$

The theoretical cross section and asymmetry formulae (equations 1.6 and 1.8) can be evaluated for the particular parameters relevant to the Qweak experiment. The relevant kinematical parameters are listed in Table 1.1.

Parameter	**Symbol**	**Value**
Beam Energy	E	1.165 GeV
Laser wavelength	λ	514 nm
Laser energy	k	2.412 eV
Compton edge	k'_{max}	48.08 MeV

Table 1.1: Parameters of the Qweak Compton Polarimeter

The wavelength of the laser is in the green range. The maximum scattered photon energy, k'_{max}, is found to be 48 MeV.

The asymmetry for Qweak parameters is depicted in Figure 1.3 as a graph of the asymmetry as a function of scattered photon energy. The graph shows the asymmetry goes to zero as the scattered photon energy goes to zero. When the photon energy is maximum, that is, at the Compton edge, the asymmetry is maximal and has a value of 0.043. The asymmetry passes through zero when the scattered photon has approximately half of the maximum energy.

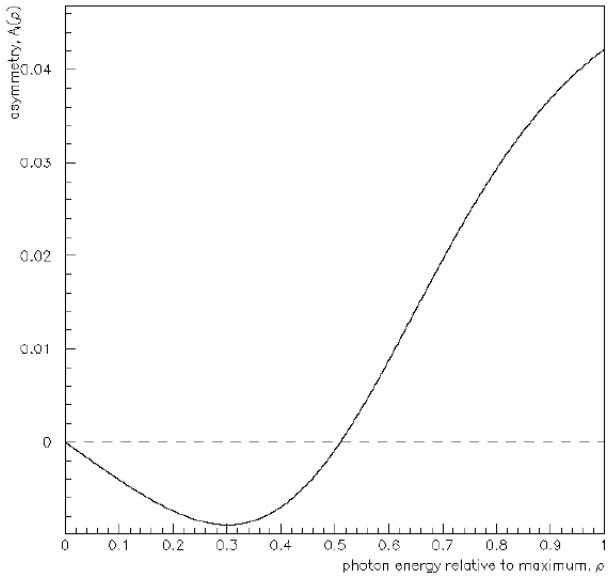

Figure 1.3: Compton Asymmetry for Qweak experiment parameters

1.3 Magnetic Chicane

A magnetic dipole chicane is used to alter the path of the electron beam. The scattered electrons must be separated from the main beam for detection. To do this, four dipole magnets arranged as shown in Figure 1.4. When electrons moving with a velocity $\vec{v}$ pass through a magnetic field $\vec{B}$, they experience a force perpendicular to both of these vectors given by $\vec{F} = e(\vec{v} \times \vec{B})$. Since the force is dependent on the momentum, or energy of the electron, those that have lost more energy from Compton scattering will be diverted more, and those with more energy will be diverted less. There exists a range of momenta from the main beam momentum to the lowest momentum, corresponding to the Compton edge. By having a detector with accurate position resolution, these electrons with various momenta can be detected separately. For Qweak, upon exiting the third magnet, the beam is diverted by 10 degrees and then drifts a distance of 2.56 meters where the scattered electrons are then detected. This distance allows the detection of scattered electrons at a minimum distance of 5 mm from the main beam [3]. The maximum distance deflected, 20.3 mm, corresponds to the Compton edge. This distance determines the size of detector needed to detect the scattered electrons.

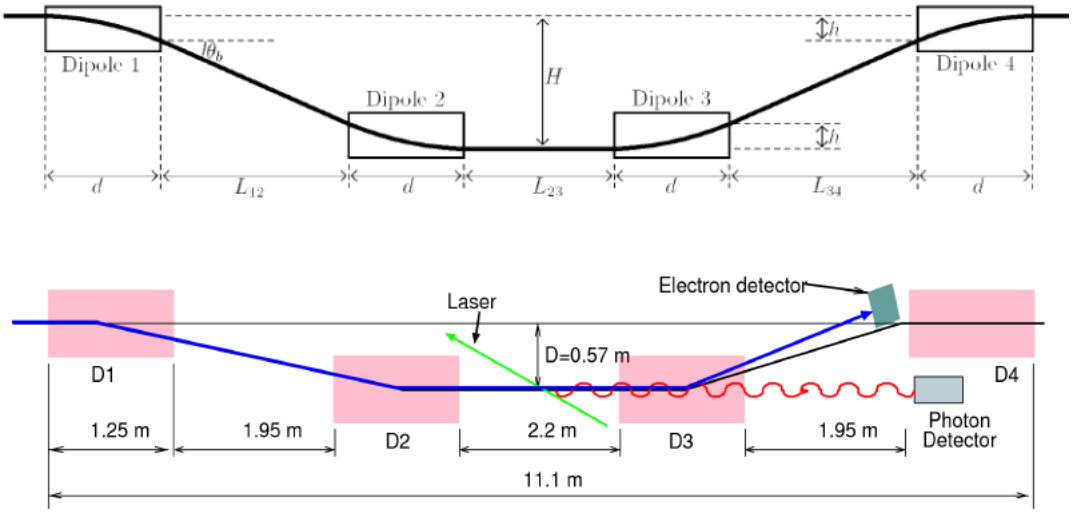

Figure 1.4: Magnetic Chicane Geometry

1.4 Electron Detection

In the Qweak Compton polarimeter, scattered electrons will be detected using a multistrip diamond detector. The detector must be able to handle high rates, as well as be radiation hard, as it will be located 5 millimetres from the main beam. In order to have a high position resolution, the detector will be a microstrip detector with gold strips arranged on the detector face with a strip pitch of 200 μm. When an electron hits the detector, it will be sensed by one of the strips, thus determining the displacement from the beam. A complete detector will consist of four planes of microstrip detectors. The distance between adjacent planes will be 1 cm. The strips will be staggered by half the strip pitch to improve the position resolution to 100 μm. The four planes will act as a coincidence such that the system will trigger if three of the four planes are hit. The combination of this and the staggering is found to give a detector efficiency close to 100% [1].

Chapter 2

Electron Detectors

The detection of particles is of central importance in experimental particle physics. Scintillation detectors use atomic excitation to create photons which are converted into an electrical signal. Semiconductor detectors however, utilize the property of the band-gap between conduction and valence bands in semiconducting materials. The incident radiation creates electron-hole pairs upon passing through the detector. These are subsequently collected by a voltage applied across the semiconductor, creating a current that is then analyzed. Diamond detectors are semiconductor detectors.

2.1 Semiconductor Detectors

Common semiconducting materials used as detectors are germanium, silicon and diamond. Semiconductors are characterized generally by their resistivity at room temperature ranging from 10^{-2} to 10^{9} ohm-cm and dependent on temperature [2]. The band gap energy between valence and conduction bands is generally around 1 eV-4 eV. In semiconductor detectors, ionizing particles deposit energy that excites electrons from the valence band of the semiconductor to the conduction band where they are free to move around. This excitation leaves a "hole" in the valence band. If a potential is applied across the semiconductor, the electrons in the conduction band are drawn to the anode and the holes are drawn toward the cathode, creating a current that can be amplified and analyzed. The number of charge carriers produced is proportional to the energy deposited in the detection medium by the ionizing radiation. Hence analysis of the detector's charge output allows for calculation of the energy deposited by the incident particles.

2.2 Silicon Detectors

Silicon is a common choice for use as a particle detector. Silicon detectors offer the advantage of high energy resolution, and the ability to be used at room temperature because of its relatively high band gap energy of 1.11 eV [2]. Silicon detectors work by employing a junction of p-type silicon (silicon doped with a group III element) and n-type silicon (silicon doped with group V element). This junction is called a diode. The p-type side has an abundance of holes, the n-type has an abundance of electrons. At the barrier, a depletion region forms from the diffusion of holes to the n-type side and the diffusion of electrons to the p-type side. Applying a voltage across the diode widens the depletion region. Ionizing radiation passes through this depletion region creating a current pulse. The reverse-biased silicon allows for a rapid transmission of the current and hence a fast time resolution.

2.3 Diamond as a Semiconductor Detector

Diamond, an allotrope of carbon, has recently emerged as a viable material for use in charged particle detection. Table 2.1 shows a comparison of some properties of diamond with silicon [4].

Property	**Diamond**	**Silicon**
Atomic Number	6	14
Density	3.52 g/cm^3	2.33 g/cm^3
Band Gap	5.5 eV	1.12 eV
Breakdown Field	10^7 V/cm	3×10^5 V/cm
Resistivity	$>10^{11}$ Ω/cm	2.3×10^5 Ω/cm
Electron Mobility	1800 cm^{2}V^{-1}s^{-1}	1350 cm^{2}V^{-1}s^{-1}
Hole Mobility	1200 cm^{2}V^{-1}s^{-1}	480 cm^{2}V^{-1}s^{-1}
Displacement Energy	43 eV/atom	13-20 eV/atom
e-h pair Creation Energy	13 eV	3.6 eV
Average Signal	36 e-h/μm	89 e-h/μm

Table 2.1: Properties of Silicon and Diamond

Carbon and silicon are both group IV elements. However, diamond's unique structure and atom size provide properties advantageous for use as particle detectors. Of note, the high band gap of diamond ensures that no excitation to the conduction band will occur as a result of thermal

energy. The diamond can therefore be used at high temperatures. The band gap and resistivity also categorize diamond as an insulator. As such, a high voltage can be applied across the diamond without electrical breakdown occuring. The same voltage would destroy a silicon detector of the same thickness. The higher mobilities of electrons and holes relative to silicon, combined with the higher voltage, allow a faster signal to be collected from the diamond. The diamond can be biased with either positive or negative voltage thereby allowing the collection of either electrons or holes. The relatively high displacement energy of diamond ensures that it is more radiation hard than silicon. The amount of energy it takes to create an electron-hole pair is related to the signal seen from the detector. Since it takes more energy to create the electron-hole pair, a smaller signal will be seen in diamond than is seen in a silicon detector. This fact is evidenced by the average signal values. Diamond is observed to have 36 electron-hole pairs produced per micron diamond, compared with 89 e-h pairs per micron in silicon. The advantages of using diamond for a detector material in the Qweak polarimeter are thus: less signal noise from thermal excitation, high radiation tolerance, and a higher rate capability due to faster signal collection. These advantages come at the expense of a lower signal.

An illustration of the detector is shown in Figure 2.1. The diamond detector works as other bulk semiconductor detectors. An incident high-energy particle creates electron-hole pairs as it passes through the detector. A bias applied to the detector allows the collection of the charge carriers, creating a current proportional to the energy of the incident particle. This current can then be analyzed and a histogram of number of particles detected for various energies created.

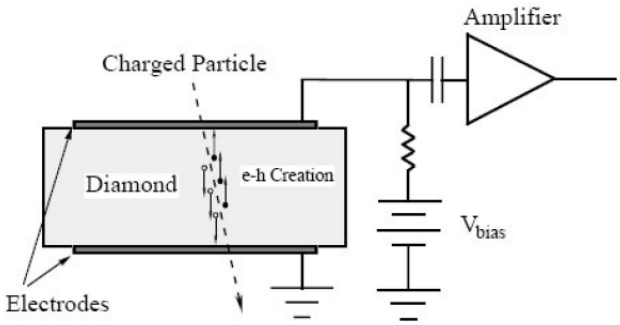

Figure 2.1: Diamond detector schematic

2.4 Microstrip Detectors

To provide the position resolution, many strips can be arranged on the surface of the semiconductor. Each of the strips can be connected to its own preamplifier. A fine strip pitch (width of unit cell) allows the position of the incident particle on the detector face to be accurately determined. The use of a microstrip detector is functionally equivalent to many detectors operated in parallel. The goal strip pitch for the Qweak Compton polarimeter electron detector is 200 μm.

Chapter 3

Experimental Setup

The University of Winnipeg is responsible for the fabrication of the diamond detector. For this, a test setup is required in order to characterize and calibrate the performance of diamonds that will be used in the detector. This apparatus was constructed and a prototype diamond was tested under various condition to study its detection properties.

3.1 Diamond Preparation

The diamond that was tested (shown in Figure 3.2) was a 0.5 mm thick, polycrystalline diamond produced by a chemical vapour deposition process. This process produces diamonds made up of multiple crystals. Upon close inspection under a microscope, it is possible to see *grain boundaries*, where the crystals come together. These can be seen in Figure 3.1. The fact that the diamond is of a polycrystalline type, as opposed to a single crystal, is a possible disadvantage, as others have reported "charge trapping" at defects in the diamond structure for single crystal diamonds [6]. The introduction of grain boundaries could potentially act as traps of charge, so that charge would be lost in the detection of particles. In addition, impurities in the diamond might create additional energy levels between the valence and conduction bands. This could also result in some of the charge being stored in these levels and not reaching the conduction band to be detected. This trapping of charge could possibly lead to a type of hysteresis effect where detector performance would depend on previous history of the detector. Some factors that might potentially affect the hysteresis might be: applied voltage, length of run time when exposed to ionizing radiation, exposure to light, and length of time between runs. These were some of the properties of the diamond that tests were

designed to examine. As well, while the diamond is 0.5 mm thick, the charge collection distance (CCD), or the average drift distance of electrons and holes [10], is around 200 μm. This distance can be measured by calibration of the diamond detector.

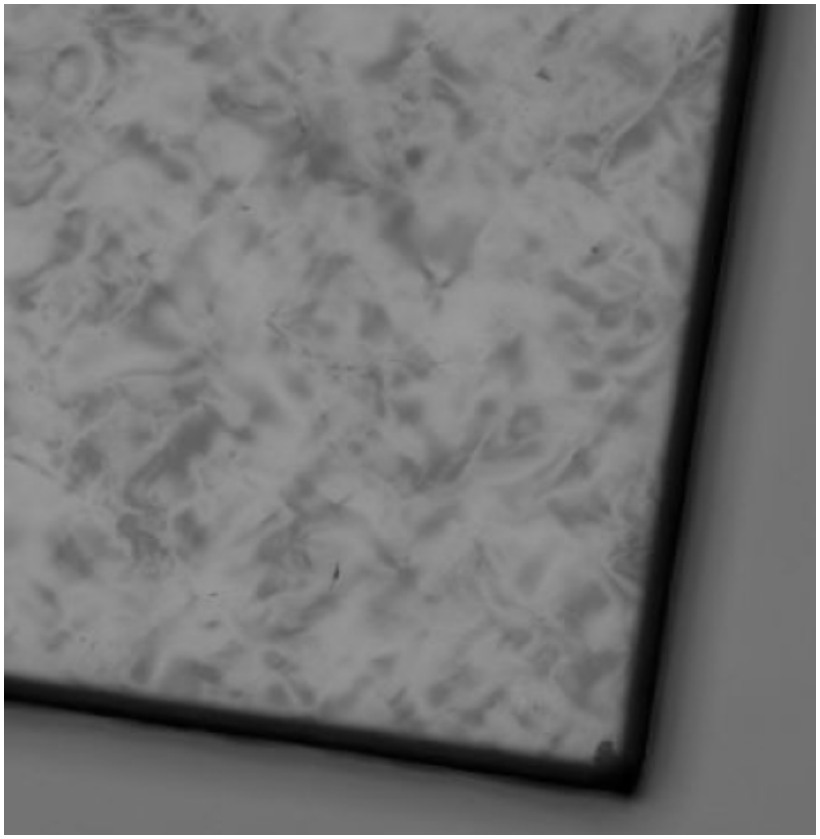

Figure 3.1: Grain Boundaries of the UWinnipeg pCVD diamond

In order to apply a voltage across the diamond, a circular electrode of gold is applied to each side of the diamond. The process by which it is applied is called sputter coating and was done at the University of Manitoba's Nanosystems Fabrication Laboratory. The gold is applied upon a thin layer of chromium, which is applied first in order to provide a surface for the gold to adhere to. Gold is chosen for many applications in electronics for its excellent conduction as well as corrosion and oxidation resistance. After being tested, the dot of gold is removed and replaced by thin strips, forming a microstrip detector, this is also able to be tested using the test setup created.

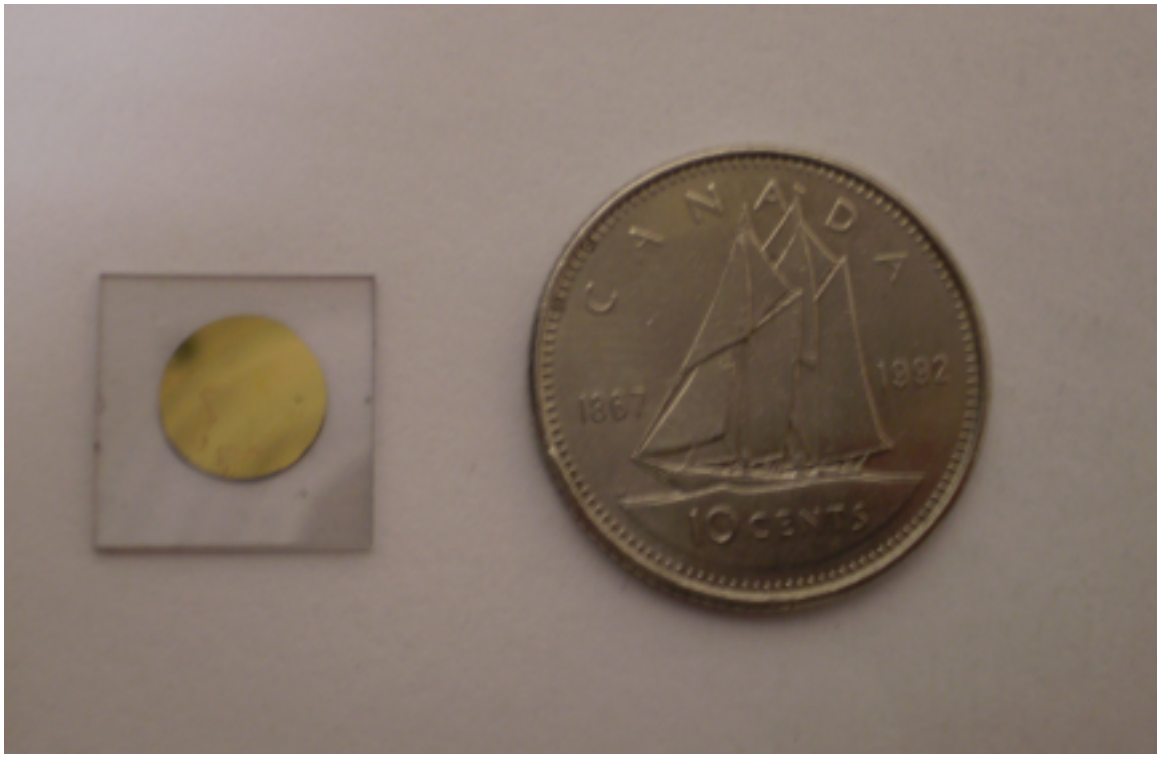

Figure 3.2: University of Winnipeg's pCVD gold coated diamond

3.2 Initial setup

The initial test setup was comprised of the diamond detector enclosure, an Ortec 109A preamplifier, connected to an Ortec 428 Dectector Bias Supply. The preamplifier output was amplified further using an Ortec 570 shaping amplifier. The resultant signal was digitized using a Tracor Northern TN-7200 multichannel analyzer (MCA). Histograms produced by the MCA could be saved to a computer for further analysis via a serial cable. The multichannel analyzer produced a histogram of number of counts for a range of channels. Each channel corresponded to a small energy range. In this way a spectra were accumulated showing the number of events detected for various energy depositions in the detecting medium. In order to achieve a pulse height of a few volts from diamond, the coarse gain on the Ortec 570 shaping amplifier was normally set at its highest setting of 1000. The experimental setup is illustrated schematically in Figure 3.3.

This setup was used to test the diamond at various bias voltages ranging from 500 to 1000 volts,

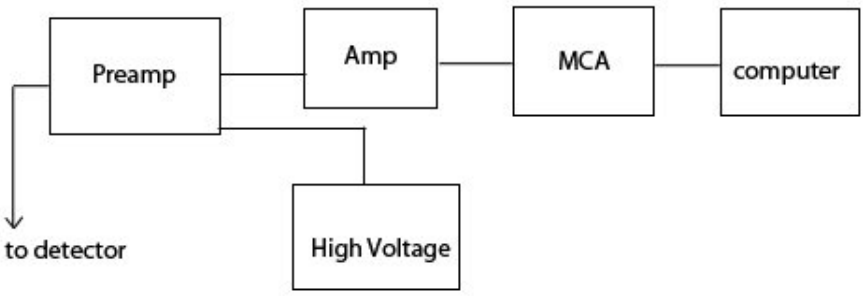

Figure 3.3: Initial Electronics Setup

both positively and negatively biased with a radioactive strontium-90 source used as a source of high-energy (∼MeV) electrons. Charged particles lose energy through interactions with other atoms in matter. The electrons detected are referred to as *minimum ionizing particles* (MIP). Minimum refers to the energy loss associated with passage through matter, that is $\frac{dE}{dx}$, or the energy loss per unit length, is a minimum. Using this source of high-energy electrons allow the diamond to be tested in a way similar its eventual application in the Qweak experiment.

3.2.1 Diamond Enclosure

The first setup used to hold and test the diamond was made at the University of Winnipeg by Doug Storey. It was constructed of an aluminum box acting as a Faraday cage, reducing the effect of external electromagnetic fields interfering with detector performance. Inside, a copper platform held the diamond sample. A copper wire contacted the top of the diamond, holding it in place and providing the applied voltage. The radioactive source was placed inside the box before it was covered. This setup was used to test the diamond, and confirm a signal could be seen, however it had drawbacks which were remedied by the fabrication of a second, improved setup. The underside of the copper platform had a grounding wire soldered to it. The solder contained lead, which severely reduces the passage of electrons. Another disadvantage to this box was it large 5 cm height was disadvantageous to use in combination with a trigger scintillator due to the amount of air the through-passing electrons would have to pass before being sensed by the trigger scintillator.

For greatest rate, the scintillator should be placed as close to the diamond as possible. In order to address these concerns, a second test setup was created, which is the final setup used for most of the results in this thesis.

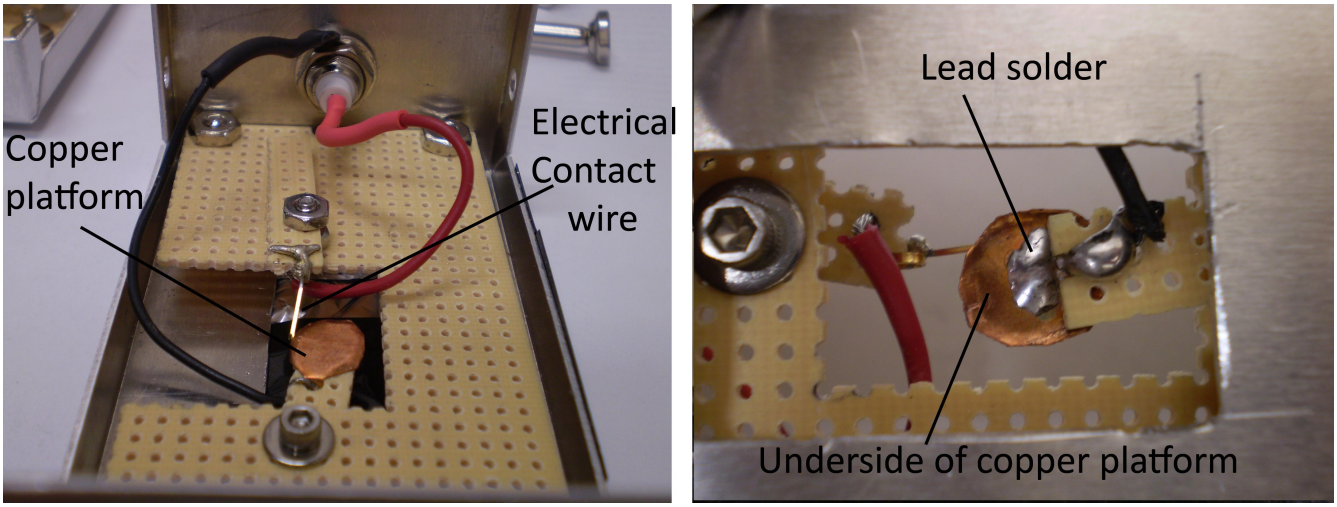

Figure 3.4: First Diamond Test Setup

The final enclosure was also fabricated at the University of Winnipeg and shown in Figure 3.5. A 5 cm x 7 cm x 1.5 cm aluminum box was used to hold the diamond. Two holes drilled on an axis through the box allow for the passage of electrons without of interacting with aluminum. One side of the diamond was placed in contact with the outer aluminum, with the gold electrode aligned over the hole to provide a direct path to effect a high probability for the incident electron to pass through the detector. A strontium-90 source was attached directly outside the hole, allowing it to be positioned a few millimeters from the diamond. The diamond was held in place firmly by a piece of circuit board. With one side of the diamond grounded to the outer metal case, the potential difference across the diamond was applied by a wire in electrical contact with the top gold electrode.

3.3 Trigger Scintillator Detector

A consequence of having a low signal from diamond is the gain on the amplifier must be increased in order to see any signal. While this increases the signal intensity, it also increases the amplitude

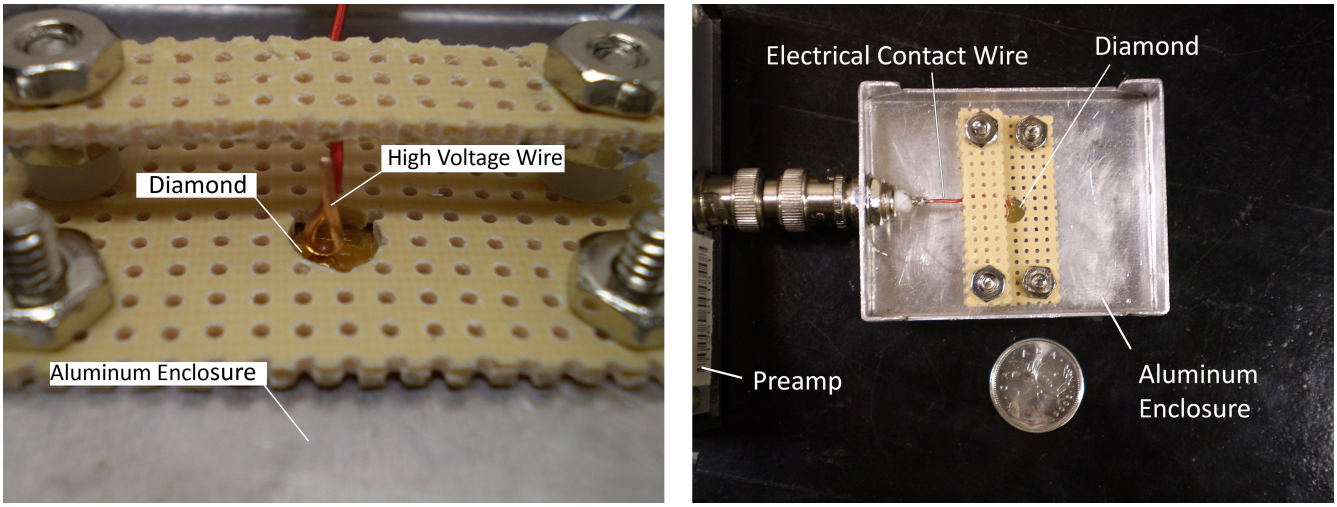

Figure 3.5: Final diamond enclosure used for calibration

of any noise present in the system. This is evident in the early tests of the diamond where no clear peak is seen. In order to detect only the minimum ionizing particles, a trigger scintillator was introduced. This was necessary since some electrons may not pass directly through the detector. These electrons will give partial energy deposition and will be digitized by the MCA, subsequently giving a spectrum that will have the peak hidden by the digitized partial energy depositions. These "bad" tracks are shown in Figure 3.7. The scintillator detector consisted of a plastic scintillator attached to a photomultiplier tube (PMT) by lightproof black plastic tape creating a thin entrance window. This scintillator detector was placed on the other side of the diamond as illustrated in Figure 3.7. It was set up such that when both the trigger scintillator and the diamond sense the presense of a minimum ionizing electron, the signal was transmitted to the MCA.

The triggering from the scintillator was achieved through the use of an Ortec 426 linear gate. The signal from the scintillator was passed into a constant fraction discriminator (Ortec 473) which outputs a logic pulse if the linear input pulse is of sufficient height. If the logic pulse is present the linear gate opens, allowing the signal from the diamond to pass through to the MCA. The coincidence of two detectors allows the reduction of most of the background noise allowing a spectrum to appear with a clear peak seen from the diamond. The schematic of the final electronics setup is illustrated in Figure 3.6.

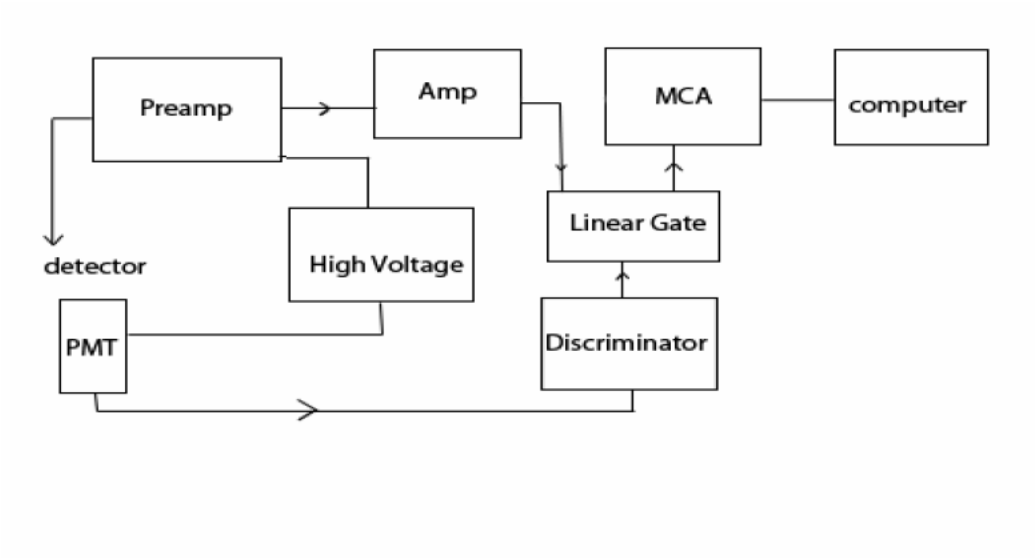

Figure 3.6: Final Electronics Setup showing inclusion of linear gate and trigger scintillator

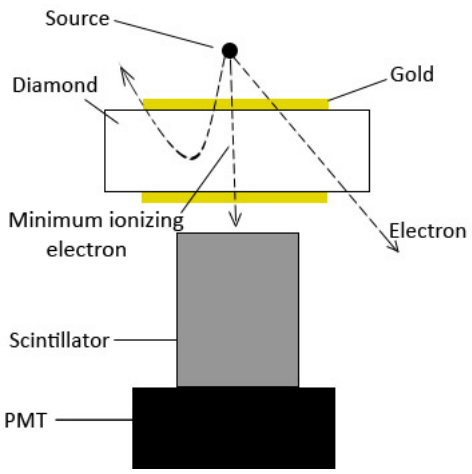

Figure 3.7: Trigger Scintillator operation

3.4 Silicon Detector

In addition to the diamond detector outlined above, an Ortec BA-035 silicon detector was used to accumulate spectra of both cesium-137 and strontium-90 sources. This detector contained silicon of 300 μm thickness. Since the average signal from silicon is much higher than with diamond, the silicon detector can be used a lower amplification while still achieve a large enough amplitude for the MCA. The spectrum of cesium-137 contains two peaks, both occuring due to conversion electrons. Conversion electrons are produced when the energy of the decaying nucleus of an atom is transferred directly to an inner shell atomic electron [7]. The conversion electrons are released with a characteristic kinetic energy. The spectra accumulated from the silicon detector allow for a calibration of the diamond detector. The energies of the particles emitted are known for both of these sources and matching the channel number of the peak to the respective energy gives a calibration of energy per channel that will also hold for diamond.

Chapter 4

Results

4.1 Silicon Detector Data

The silicon detector serves two purposes. A signal seen from the detector confirms the electronics are functioning correctly before proceeding with testing the diamond. Secondly, spectra accumulated with this detector lead to a calibration of the electronics chain, relating energy deposited in the detector to channel number in the multi-channel analyzer. Energy calibration is necessary in order to calculate particle energies, electron-hole pairs captured, and charge collection distance for the diamond detector data. The diamond detector results can then be more readily compared with results from other groups who have tested diamonds for the purpose of charged particle detection, and hence confirm the functionality of the diamond quantitatively.

Figure 4.1 shows the silicon detector spectra accumulated for exposure to cesium-137 and strontium-90 radioactive sources. The cesium plot shows two conversion electron peaks of 624 keV and 656 keV at channel 1800 and 1875 respectively. The flat portion of the spectrum before the conversion peaks occurs from the beta endpoint of cesium which is 514 keV. The decay of cesium-137 produces a 662 keV photon. This does not appear on the plot as the silicon is too thin to allow much interaction with this photon. However, photons can scatter from electrons in the silicon giving some additional low-energy deposition in silicon. The spectrum shows an increase in counts as channel number decreases due to beta and gamma particles from the cesium source depositing various energies in the silicon. A small amount of noise is seen at the beginning of the spectrum that was not cut out when digitized by the MCA. From fitting a Gaussian curve to the larger of the two peaks, the peak corresponding to the 624 keV conversion electron of cesium occurs at channel

1800. This gives an energy calibration of 0.35 keV/channel.

The strontium source has no photons emitted. The isotope strontium-90 decays to yttrium-90 via beta decay. The endpoint energy for the decay is 546 keV. The strontium spectrum shows a clear peak from the minimum ionizing beta particle with a long tail due to lower energy particles. The slight shoulder observed in the spectrum between channels 700 and 1000 is most probably due to the 546 keV beta endpoint of strontium.

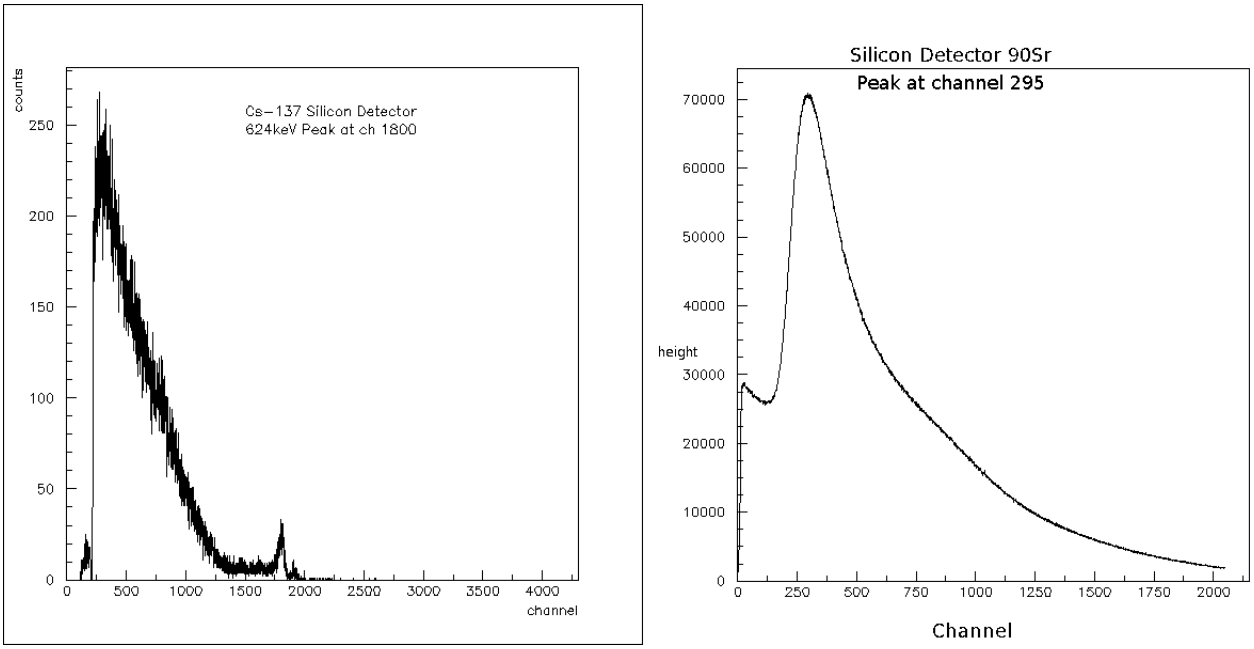

Figure 4.1: Spectra accumulated from silicon detector for Cesium-137 (left) and Strontium-90 (right)

4.2 Diamond Calibration Methodology

Having the energy calibration from silicon allows properties of diamond to be calculated. Specifically, knowing the peak channel from the spectra taken from diamond allows the calculation of number of electron-hole pairs collected, energy deposited in the detector, and charge collection distance. The relationship of data to these quantities will now be explained.

The energy deposited in a detection medium by a minimum ionizing particle is given by,

$$\Delta E = \frac{dE}{dx}\rho t. \tag{4.1}$$

Here, ΔE is the energy deposited in the material by the incident radiation, $\frac{dE}{dx}$ is the energy loss of the MIP (alternatively the "stopping power" of the material), ρ is the density of the material, and t is the thickness over which charge is collected (CCD). For silicon, the CCD is the detector thickness. For diamond, the CCD is less than the detector thickness due to the trapping centers created by grain boundaries and impurities. The stopping power is specific for the material through which the incident particle passes, as well as the energy of the incident particle. Tables exist where these values have been tabulated for many materials [11]. The above formula is an approximation valid for thin, planar detectors. That is, it assumes $\frac{dE}{dx}$ is approximately constant as the particle passes through the detector.

To calculate the number of electron-hole pairs created, we can use the energy calibration from silicon,

$$\text{(number of e-h pairs)} = N_{eh} = \mathscr{C} \cdot G \cdot E_{eh} \tag{4.2}$$

where $\mathscr{C}$ is the energy calibration from silicon, G is the relative gain factor of the amplifier, and E_{eh} is the energy required to create an electron-hole pair in the specific material. The coarse gain knob on the amplifier was normally set to 50 for the silicon detector while for diamond it was normally set to 1000. G allows this change to be taken into account, assuming no zero-offset. Knowing the number of electron-hole pairs created is equivalent to knowing the energy deposited since the energy to create an electron-hole pair is known.

From silicon, using the same relative gain setting so that G=1, we have $\mathscr{C} = 0.35\frac{\text{keV}}{\text{ch}}$. This corresponds to 97 electrons/channel, using the energy to create an electron-hole pair in silicon which is 3.6 eV from Table 2.1. From a Gaussian fit to the 90-Sr spectrum in Figure 4.1, the peak occurs at channel 295. For the energy deposited in silicon from 90-Sr, we then have $295 \times 0.35\frac{\text{keV}}{\text{ch}} \approx 100$ keV. This can be checked using the tables of energy losses for silicon. From the table, the minimum stopping power is 1.5 $\frac{\text{MeV cm}^2}{\text{g}}$. Knowing the thickness of the detector to be 300 μm, and the density of silicon (2.33 g/cm^3), Equation (4.1) yields approximately 100 keV. The fact that the measured number agrees with the number calculated based on stopping power indicates that the stopping power and Equation (4.1) are valid for the silicon detector.

Considering diamond, the spectrum with the largest signal for 1000V applied voltage is shown

in Figure 4.3. The mean in the MIP peak in the spectrum occurs at channel 1970. The mean channel was calculated using

$$\bar{c} = \frac{\sum_i c_i N_i}{\sum_i N_i} \tag{4.3}$$

where c is the channel, N is the number of counts. The sum was performed over the peak. Since the mean energy deposition is often the quantity of interest, it is the mean channel number that is used in the calculations.

We had previously, 97 electrons/channel for coarse gain setting setting on the amplifier being 50 for silicon. For diamond, the coarse gain knob was set to 1000, thus G=20 if we wish to use the silicon data to calibrate the diamond data. The factor 97 e^-/ch then becomes 4.9 e^-/ch for diamond data. We then have for the number of electrons collected, $4.9\frac{e^-}{ch} \times 1970 \approx 9600$ electrons collected.

Again, this can be compared with results from the table of energy losses. For carbon, the minimum stopping power is listed as 1.6 $\frac{\text{MeV cm}^2}{\text{g}}$. Using an estimate of 200 μm as the CCD, and the density of diamond, 3.52 g/cm^3, Equation (4.1) gives about 113 keV deposited. Using the energy to create an electron-hole pair in diamond, 13 eV from Table 2.1, this corresponds to around 8700 electrons expected. From this, it may be deduced that our CCD is in fact somewhat larger than 200 μm. For similar tests of diamond at Ohio State University, at 1000V a CCD of 230 μm was determined.

Using the result of 9600 electrons collected and inverting Equation (4.1) to solve for the CCD, we therefore find the CCD of the diamond at 1000V to be 220 μm.

To summarize, calibration of the electronics using the silicon detector allows one to measure the number of electrons (or holes) collected for diamond in a straightforward manner. Further inference of the CCD is possible using energy loss tables. Confidence in the procedure is gained from the excellent agreement for the Sr-90 minimum ionizing peak in silicon with the calculation based on energy loss tables. The following sections study diamond results with the understanding that the following calibration factors hold: 1 channel = 4.9 electrons (or holes)= 64 eV = 0.14 μm.

These understandings are not without some caveats. First, the accuracy of the gain knob implies a validity at the 5% level. That is, the increase of amplifier gain from 50 to 1000 may not be an exact increase by a factor of 20. The zero offset of the amplifier, as will be discussed in Section 4.4, a shift of about 100 channels is observed when switched from positive to negative. Taking an typical signal size of 1600 channels, this implies an typical error from zero offset of around 6%.

Also, the assumption of constant $\frac{dE}{dx}$, which would be the case for an infinitesimally thin diamond, implies the electron is no longer minimum ionizing by the time it traverses the thickness of the detector. Since ΔE is a significant fraction of the initial energy, this approximation implies some degree of error. Additionally, after the electron passes through the diamond, the energy loss in air before it is detected at the scintillator is assumed to be negligible. This may not be the case in all situations as the electron may not necessarily make it to the scintillator. The wide peak in Figure 4.3 occuring because of the energy loss implies the width of the peak can be regarded as the uncertainty in energy loss. From the width of the peak (given by twice the standard deviation of 640 channels found from a Gaussian fit to the peak), a validity at the 30% level is estimated.

Taking all of these into account, the dominant effect is that of the constant $\frac{dE}{dx}$. When added in quadrature, the other effects contribute minimally. We then conclude conservatively, that the calibration results are good to the 30% level. To do much better would require a detailed Monte Carlo simulation of the entire test setup.

4.3 Diamond in self-triggered mode

The initial tests of diamond were performed in self-triggered mode. That is, the pulse height from the amplifier was digitized if it exceeded a threshold. The results confirm that there is a signal from the diamond, however the high noise level and low rate prevents a clear MIP peak from being seen in the spectrum. Instead, a noise peak is seen and a shoulder appears approximately where the peak is expected. This can be seen in Figure 4.2 where several spectra are presented. The MIP shoulder is indicated approximately by the vertical dashed line in the plot. In self-triggered mode, the output signal of all electrons that deposit charge is digitized. Some of these electrons may not pass directly through the diamond, and hence contribute only partial charge deposition. This is consistent with incomplete charge collection that would tend to fill the valley below the already broad minimum ionizing peak. The collimation and introduction of the trigger scintillator is then the way to proceed in order to digitize only the minimum ionizing particles. Despite these issues with collimation and triggering, as the voltage is changed, the shoulder in the spectrum is observed to shift. The shift is consistent with more electrons (or holes) being collected as increased bias voltage is applied to the detector. Figure 4.2 a) shows this behavior for an initial test of diamond. From the plot, the shoulder seen is observed to shift to higher channel number for increased voltage. This is indicative of more electrons being collected for higher applied bias voltage.

Figure 4.2 b) shows multiple runs over different days at 1000 volts. The graph shows all the

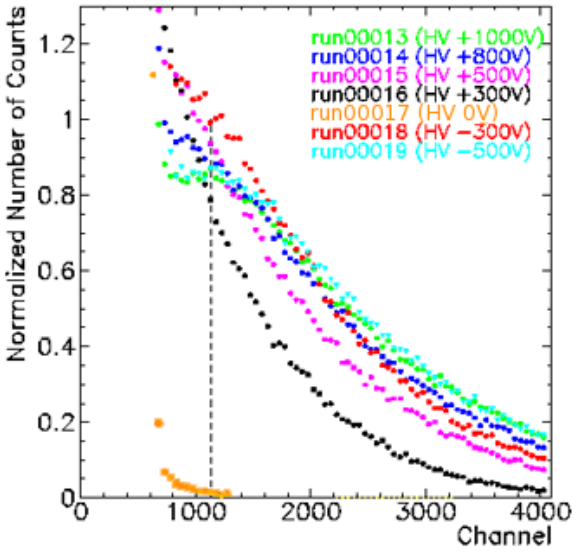

a) Diamond detector tests at various voltages without trigger scintillator

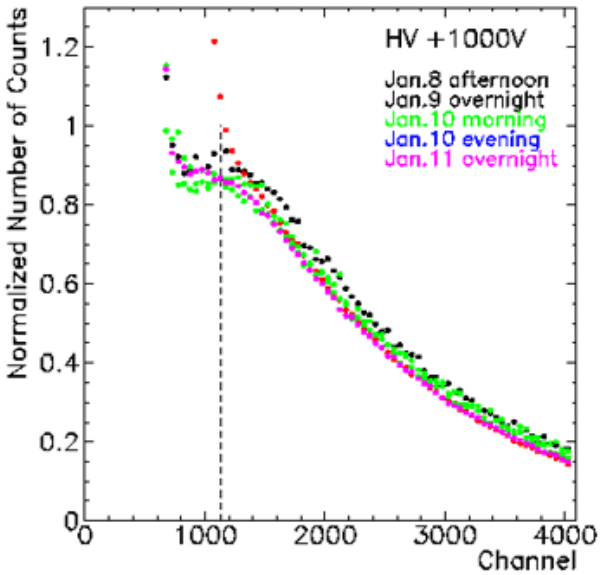

b) Diamond detector tests at 1000V without trigger scintillator

Figure 4.2: Diamond detector tests without trigger scintillator

shoulders of the peaks line up consistently, indicating the diamond response was not strongly time dependent over runs ranging in length from 2 hours to 17 hours, and acquired over the course of four days.

4.4 Diamond With Trigger Scintillator

With the addition of the trigger scintillator, the backgrounds were significantly reduced so that a clear MIP peak could now be seen in the diamond detector spectra. Figure 4.3 shows a typical Sr-90 spectra accumulated using the diamond detector. The features of the spectrum are a clear minimum ionizing peak (where a curve has been fitted to estimate the most probable energy loss), and distribution given by fluctuation in energy loss from other incident electrons passing through the diamond. At very low channels, an increase in number of counts is seen due to noise.

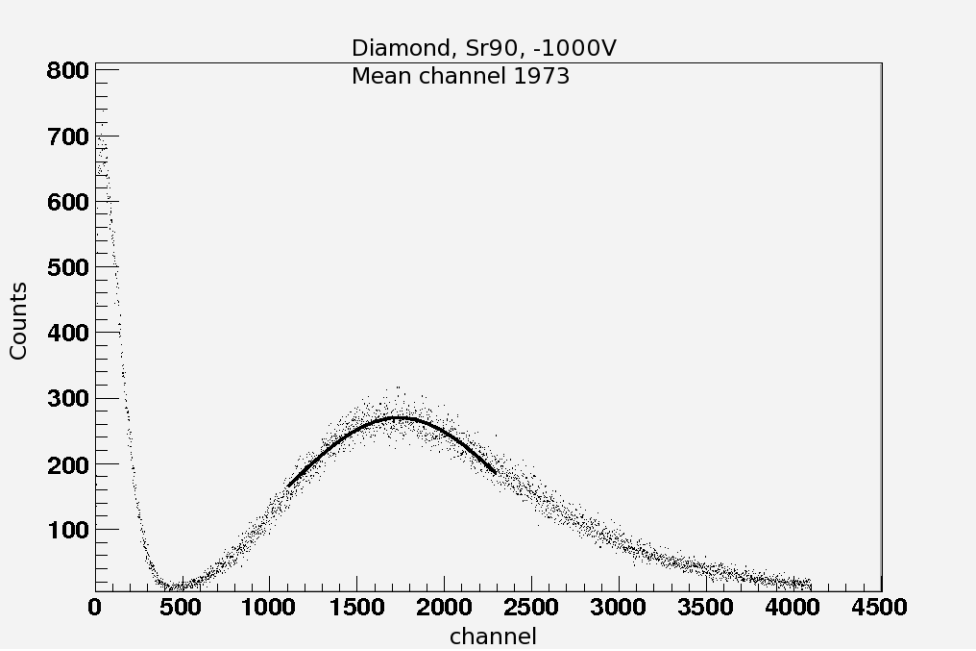

Figure 4.3: Strontium 90 Spectrum accumulated using diamond biased at -1000V with trigger scintillator

To test for a possible hysteresis effect, the diamond was systematically tested at different voltages, both positive and negative. The results of these tests are shown in Figure 4.4, where the mean

channel determined by Equation 4.3 is plotted against the run number. Run number indicates time ordering. The results show an increase in mean channel with increased voltage, and when the voltage is brought back to initial levels, no significant change in mean channel is observed. The observed change of approximately 100 channels between the same voltage of different polarity is accounted for by a baseline shift of approximately 0.2 volts when the amplifier is switched from positive to negative. Hence, holes and electrons give equal results to within error. From the tests, it can be concluded that there is no significant hysteresis effect with the diamond.

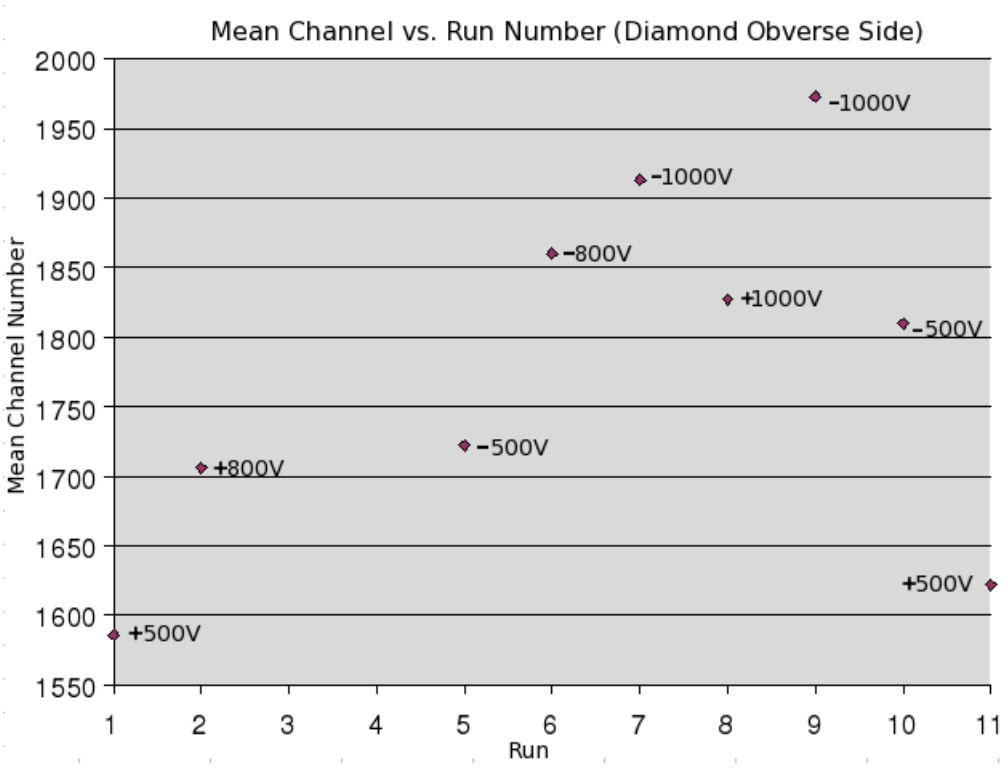

Figure 4.4: Summary plot of mean channel of spectra for various voltages. Obverse side of diamond.

A similar test was performed on the reverse side of the diamond. The results are shown in Figure 4.5. As with the obverse, the reverse side performs identically, with no signs of hysteresis although lower overall signal is seen, indicated by lower mean channels. This could be due to factors such as poorer diamond crystal quality, poorer electrode quality, or poorer electrical contact. However, results are relatively consistent.

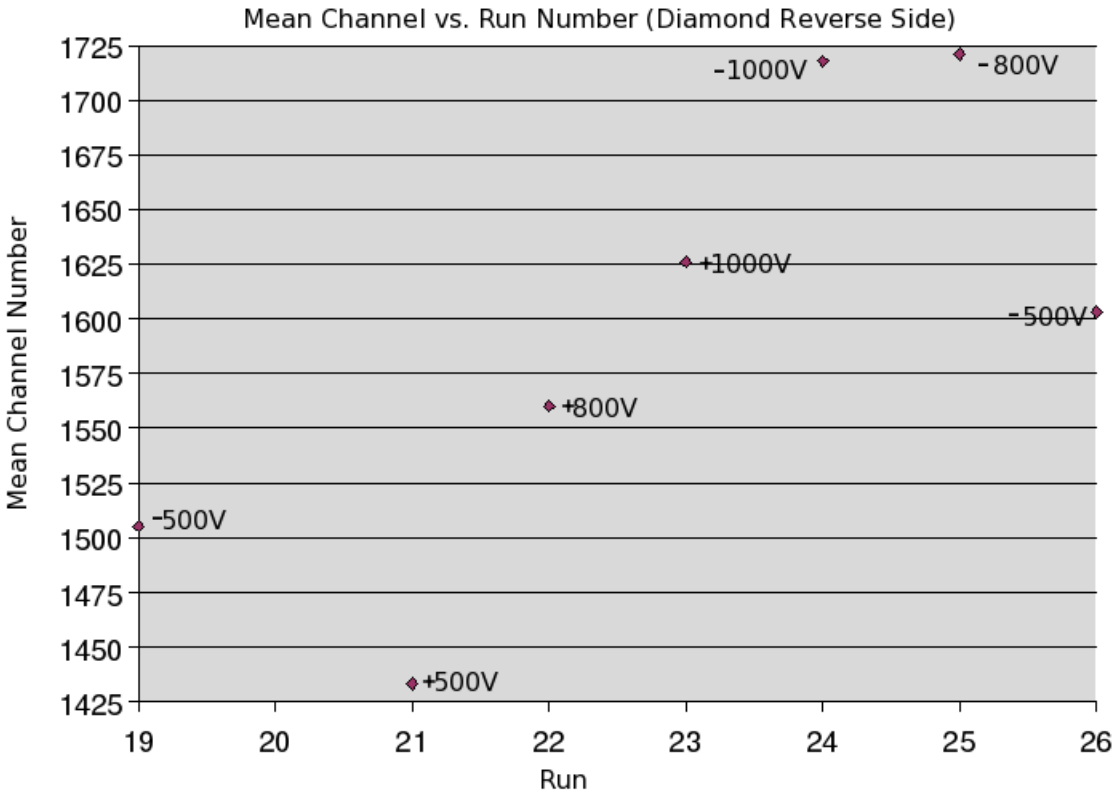

Figure 4.5: Summary plot of mean channel of spectra for various voltages. Reverse side of diamond.

The diamond was also tested to characterize the stability of the signal over an extended period of time. For this, the diamond was run for seven days continuously at +1000V. The result of the test showed no degradation of the signal after this time period.

4.4.1 Performance under exposure to light source

The location of the electron detector in the Qweak Compton polarimeter will not be free of light. There will exist synchrotron radiation in the beam pipe. This radiation is produced when the electrons are accelerated passing through the dipole magnets and is comprised of photons mostly in the visible region of the electromagnetic spectrum [3]. This radiation can cause problems to the electron detector. The ability for the detector to perform with exposure to light was examined in tests. Light exposure to diamond may influence the charge trapping centers giving a time dependence as the traps empty and fill. To test the diamond exposed to visible light, the top cover of the diamond enclosure was removed and a 100 W, tungsten filament light was placed approximately 10 cm from the diamond. The trigger scintillator was kept in its usual position above the diamond. The diamond was tested for 1.5 hours under these conditions, at both +1000V and at +800V. The diamond performed stably under these conditions, with peak position in accordance with previous trials run in near-dark conditions.

4.4.2 Performance with different cable lengths

When used in Qweak, the diamond detector will not be connected directly to the preamplifier. Instead it will be connected by a shielded cable. In order to characterize the signal changes with the addition of the cable, tests were run using different length cables connecting the diamond detector to the preamplifier. Figure 4.6 shows the results for various cable lengths tested.

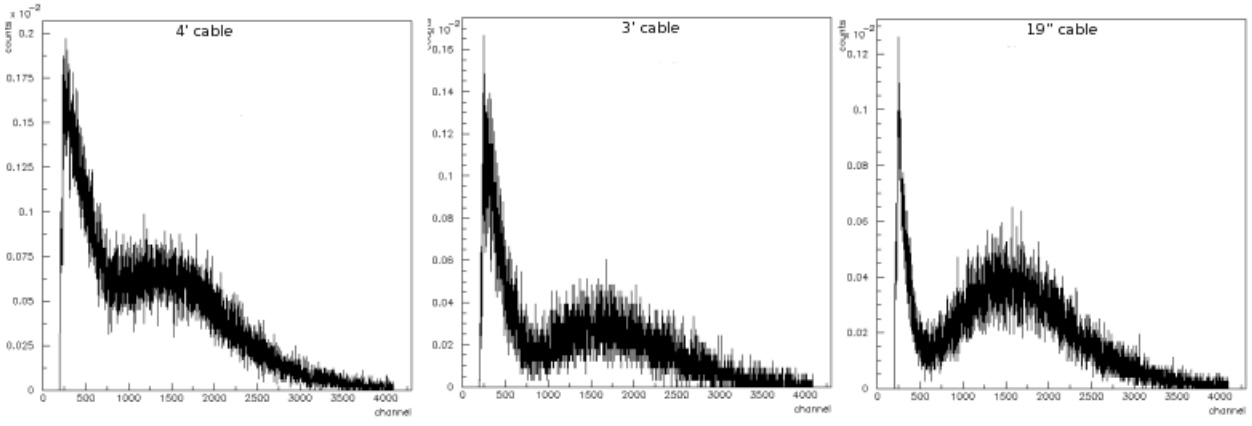

Figure 4.6: Test of various cable lengths to preamplifier

From this, the peak to valley ratio is seen to decrease with cable length. The conclusion of this test is that a cable of two feet (the cable length envisioned for Qweak) can be used without degrading the signal-to-noise ratio significantly.

4.5 Diamond Microstrip

After successfully testing the performance of the diamond, the circular gold electrodes were removed, and replaced by finely spaced gold readout strips, as a test of the fabrication technique eventually to be used to construct the final detector for the Compton polarimeter. The strips had the design pitch of 200 μm, and were comprised of 180 μm strips separated by 20 μm. To test the success of the application of the strips, the microstripped diamond was tested in the setup. The diamond was positioned with the strips in contact with the outer aluminum and tests were run at both positive and negative voltages.

A spectrum accumulated from one of the tests is shown in Figure 4.7. It exhibits the same features of the plot shown previously for the diamond tested with both circular electrodes (Figure 4.3). The MIP peak occurs at channel 810, indicating half the previous signal seen with both circular electrodes. The same low channel noise and tail that were previously seen are observed.

While the signal is not expected to be less, possible re-positioning of the diamond in the setup to produce better electrical contact could improve the result. It was therefore concluded that the fabrication process had resulted in a functioning detector device. Based on this information, the detector was attached to a carrier board by silver epoxy, and wirebonded. This is shown in Figure 4.8. The next step in the process is use the same basic technique with multi-strip electronics.

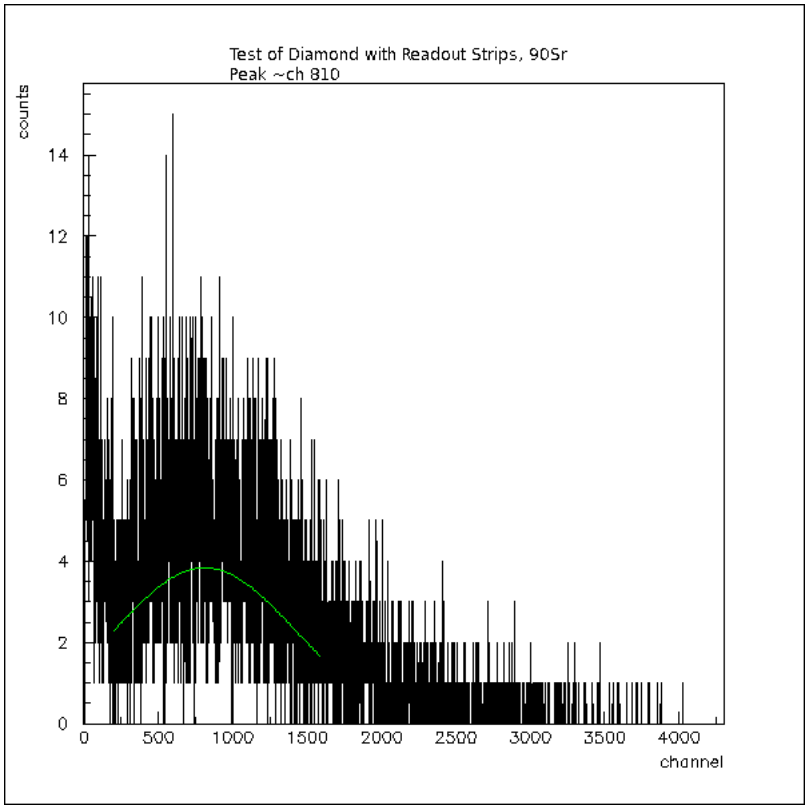

Figure 4.7: Spectrum accumulated from microstripped diamond

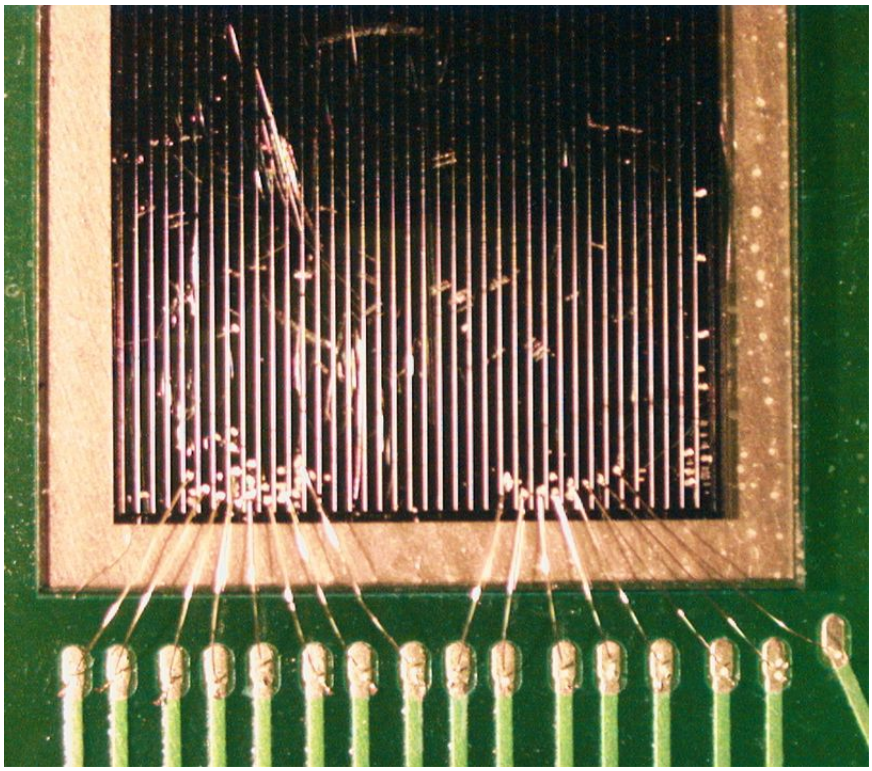

Figure 4.8: Microscope photograph of microstripped diamond mounted to green printed circuit board showing wire bonds to traces on PCB

Chapter 5

Conclusion

The theory of Compton polarimetry and semiconductor diamond detectors has been discussed and the test setup constructed at University of Winnipeg to test diamond was described. A prototype diamond similar to that which will be used in the Qweak experiment Compton polarimeter was successfully tested and calibrated using this setup. By a cross-calibration with a silicon detector, the number of electron-hole pairs created in diamond by the deposition of energy by a minimum ionizing particle was calculated to be 9600 for 1000V applied voltage, in accordance with other group's tests of diamond as a detector medium. Further tests show no effect on performance from exposure to a light source, an important result as there will be synchrotron radiation in the Qweak beam pipe. Tests of long-term stability confirm no signal degradation over an extended run time period of one week. As well, tests using various cable lengths connecting the diamond to the preamplifier show that a two foot cable, as envisioned for the Qweak detector, can be used without a significant increase in the signal-to-noise ratio. A test of the microstripped diamond in the test setup confirmed the process of application of gold microstrips to be a success.

Having developed a working procedure to test and calibrate diamonds, future steps will include using the same technique to test gold microstripped diamonds using multi-channel electronics. The culmination of the tests will be the Qweak experiment, set to begin installation at Jefferson Lab in late 2009.

Bibliography

[1] J.W. Martin, "Some Design Considerations for the Hall C Compton Electron Detector", University of Winnipeg (2006).

[2] C. Kittel, *Introduction to Solid State Physics*, John Wiley and Sons, New Jersey (2005).

[3] G. Bardin *et al*,"Conceptual Design Report of a Compton Polarimeter for Cebaf Hall A" (1996)

[4] M. Breidenbach *et al*, "Diamond Detectors", NLC - Next Linear Collider Presentation (2004), accessed from www.slac.stanford.edu/xorg/lcd/ipbi/monthlymeetings/02jun2004/DiamondDetectors.pdf.

[5] B. Campbell *et al*, "Lattice damage caused by the irradiation of diamond", Nuclear Instruments and Methods in Physics Research A 476 (2002), 608-685.

[6] M. Pomorski *et al*, "Charge transport properties of single crystal CVD-Diamond particle detectors", Diamond and Related Materials 16 (2007) 1066-1069.

[7] C. Delaney and E. Finch, *Radiation Detectors*, Oxford University Press, New York (1992).

[8] W. Adam *et al*. "The development of diamond tracking detectors for the LHC", Nuclear Instruments and Methods in Physics Research A 514 (2003) 79-86.

[9] W. Adam *et al*, "Radiation tolerance of CVD diamond detectors for pions and protons", Nuclear Instruments and Methods in Physics Research A 476 (2002) 686-693.

[10] E. Berdermann *et al*, "Charged particle detectors made of single-crystal diamond", Phys. Stat. Sol. (a) 201 No.11 (2004) 2521-2528

[11] L.G. Greeniaus, "TRIUMF Kinematics Handbook", second edition, TRIUMF, Vancouver, Canada. (1987), available at http://www.triumf.ca/triumf-handbooks/.